



Thermal Transport in Electrospun Vinyl Polymer Nanofibers: Effects of Molecular Weight and Side Groups

Journal:	<i>Soft Matter</i>
Manuscript ID	SM-ART-08-2018-001696.R1
Article Type:	Paper
Date Submitted by the Author:	10-Oct-2018
Complete List of Authors:	Zhang, Yin; Southeast University, Mechanical Engineering Zhang, Xin; Vanderbilt University, Mechanical Engineering Yang, Lin; Vanderbilt University, Mechanical Engineering Zhang, Qian; Hermes-Microvision Inc., ; Vanderbilt University College of Arts and Science, Mechanical Engineering Fitzgerald, Matthew; Vanderbilt University, Mechanical Engineering Ueda, Akira; Fisk University, Center for Physics and Chemistry of Materials Chen, Yunfei; Southeast University, Mechanical Engineering Mu, Richard; Tennessee State University, TIGER Institute Li, Deyu; Vanderbilt University, Mechanical Engineering Bellan, Leon; Vanderbilt University, Mechanical Engineering

Thermal Transport in Electrospun Vinyl Polymer Nanofibers: Effects of Molecular Weight and Side Groups

Yin Zhang^{1,2 †}, Xin Zhang^{2 †}, Lin Yang^{2 †}, Qian Zhang², Matthew L. Fitzgerald², Akira Ueda³,

Yunfei Chen¹, Richard Mu^{4}, Deyu Li^{2*}, Leon M. Bellan^{2*}*

¹Jiangsu Key Laboratory for Design and Fabrication of Micro-Nano Biomedical Instruments, School of Mechanical Engineering, Southeast University, Nanjing 211189, China.

²Department of Mechanical Engineering, Vanderbilt University, Nashville, TN 37235, USA.

³Center for Physics and Chemistry of Materials, Fisk University, Nashville, TN 37208, USA.

⁴TIGER Institute, Tennessee State University, Nashville, TN 37209, USA

†: These authors contributed equally to this work

*: Author to whom correspondence should be addressed.

E-mails: rmu@tnstate.edu; deyu.li@vanderbilt.edu; leon.bellan@vanderbilt.edu

Abstract: Understanding and enhancing thermal transport in polymers is of great importance, and is necessary to enable next-generation flexible electronics, heat exchangers, and energy storage devices. Over the past several decades, significant enhancement of the thermal conductivity of polymeric materials has been achieved, but several key questions related to the effects of molecular structure on thermal transport still remain. By studying a series of electrospun vinyl polymer nanofibers, we investigate the relationship between thermal conductivity and both molecular chain length and side group composition. For polyethylene nanofibers with different molecular weights, the measured thermal conductivity increases monotonically with molecular chain length, as energy transport along molecular chains is more efficient than between chains. The observed trend is also consistent with structural characterization by Raman spectroscopy, which shows enhanced crystallinity as molecular weight increases. Further, by comparing the measured thermal conductivity of vinyl polymer nanofibers with different side groups, we found that phonons travel along polymer chains more effectively when the side groups are either lighter or more symmetric. These experimental results help reveal the underlying correlation between the molecular structure and thermal conductivity of polymer nanofibers, providing valuable insights into the design of polymeric materials with enhanced thermal conductivity.

Keywords: Vinyl polymer nanofibers, electrospinning, thermal conductivity, molecular weight, side groups

Introduction

Polymers are an important class of materials due to their desirable and tunable properties, abundance, and low cost. A long-standing issue for polymeric materials that limits their applications in many fields is their extremely low thermal conductivities (on the order of $0.1 \text{ W m}^{-1} \text{ K}^{-1}$), which is due to the random network formed by the carbon backbone and the weak inter-chain interactions mediated by weak van der Waals forces. This leads to poor heat dissipation that largely restricts polymer usage and imposes severe limitations in various applications such as light-emitting devices,^{1,2} photovoltaic cells,^{3,4} and flexible thin-film transistors.^{5,6} To address this issue, a significant amount of efforts have recently been dedicated to enhancing the thermal conductivity (κ) of polymeric materials.⁷⁻¹³

It is well-known that the low thermal conductivity of most polymeric materials is a result of their molecular structure generally consisting of coiled-up chains entangled together. The thermal conductivity along individual molecular chains, however, can actually be quite good because of the strong intra-chain covalent bonding between atoms. In fact, a recent molecular dynamics (MD) simulation⁷ has suggested that an isolated single polyethylene (PE) molecule may possess very high thermal conductivity, up to $\sim 350 \text{ W m}^{-1} \text{ K}^{-1}$. Inspired by this prediction, several experimental efforts have focused on enhancing the thermal transport properties of polymer nanofibers with aligned molecular chains.^{8,12,14-16} The highest experimentally measured thermal conductivity of a polymeric material was reported by Shen et al.,⁸ who reported on single ultra-drawn PE nanofibers with thermal conductivity values as high as $\sim 104 \text{ W m}^{-1} \text{ K}^{-1}$. This dramatic enhancement of thermal conductivity is due to the fact that small crystallites, split from the crystalline lamellas and connected by microfibrils, are aligned along the fiber axis during the drawing process, yielding a high degree of molecular orientation.⁸

Electrospinning has become a popular approach to prepare nanofibers for various applications, with polymers being the most common type of materials used for electrospun fiber production. During electrospinning, a strong electric field forces a liquid jet from a droplet of dissolved polymer chains, and a continuous nanofiber is formed as the solvent evaporates in flight. The strong elongational flow in this jet often results in fibers with substantial molecular orientation, which may lead to significantly enhanced thermal conductivity along the fiber direction. For example, it has been shown that the thermal conductivity of single Nylon-11 electrospun fibers may be as high as 1.6 W/m-K, nearly one order of magnitude higher than the typical bulk value of ~ 0.2 W/m-K.¹⁴ In addition, Canetta et al. measured the thermal conductivity of individual electrospun polystyrene nanofibers, obtaining values ranging from 6.6 to 14.4 W/m-K, a significant increase from typical bulk values.¹⁶ Ma et al. recently showed that the thermal conductivity of electrospun PE nanofibers may be as high as $9.3 \text{ W m}^{-1} \text{ K}^{-1}$ at 300 K, over 20 times higher than the bulk value, an increase that was attributed to ordered molecular chain alignment and enhanced crystallinity as indicated by Raman spectroscopy.¹²

In addition to chain alignment and crystallinity, polymer topology and morphology has also been demonstrated to affect the thermal conductivity of polymeric materials.^{17,18} For example, a recent MD simulation has shown that longer side chain of bottlebrush polymers will increase interchain phonon scattering and decrease the thermal conductivity;¹⁷ and for π -conjugated 2D polymers, the calculated lower thermal conductivity with increasing porosity is attributed to the increased chain disorder and segmental rotation.¹⁸ While notable progress has been made, several key questions related to the effects of molecular structure on thermal transport in electrospun polymer nanofibers still remain to be answered. For example, no experimental study has been done to investigate the effects of molecular weight (i.e. chain length) and side groups on thermal

transport in individual electrospun polymer nanofibers. In this paper, we show how these two factors influence the thermal conductivity of electrospun vinyl nanofibers, which share the same planar-zigzag carbon backbone. Given that electrospinning has become a widely-adopted approach to produce large amount of polymer nanofibers, this study could provide knowledge to fine tune the electrospinning process to obtain high thermal conductivity electrospun polymer nanofibers.

Sample Description

To investigate the effects of molecular weight (M_w) and side groups, we prepared four different kinds of electrospun vinyl nanofibers: PE, polyvinylidene fluoride (PVDF), polyvinyl alcohol (PVA) and polyvinyl chloride (PVC). Based on the PE powders that were commercially available, we fabricated PE nanofibers with four different M_w (chain lengths), namely 35,000, 125,000, 420,000, and 3,000,000 (Supporting Information). For the other three materials used, we tried to keep the chain length as similar as possible (as listed in Table 1). These vinyl polymers have similar chain structures (Fig. 1a), with identical carbon backbones but different side group atoms. Since it has been shown that the electric field strength in the electrospinning process plays a critical role in the thermal conductivity of resulting PE nanofibers,¹² in this study we adopt fixed values for both the applied voltage (30 kV) and the distance (15 cm) between the syringe tip and the collector to keep the electric field constant, as shown in Fig. 1b. Fig. 1c shows a high magnification scanning electron microscopy (SEM) micrograph of an individual electrospun PVDF nanofiber. During the electrospinning process, the nanofibers can be collected on silicon chips that have pre-patterned trenches (Fig. 1d) for micro-Raman studies and Young's modulus characterization. For thermal conductivity characterization, the fibers were collected with a piece

of polydimethylsiloxane (PDMS) to facilitate subsequent sample transfer to the measurement device (Fig. 1e), which was then measured following a well-established approach.^{19–23} As it has been shown that storage in a vacuum chamber can help to remove solvent residues,¹² all fibers were kept in a vacuum chamber overnight prior to any measurements.

Results and discussion

Fig. 2a shows the measured thermal conductivity for PE nanofibers composed of molecular chains with four different values of M_w . For each M_w , we tested three samples, and it can be seen that even though some variations exist for samples within each group, there is a clear trend of higher thermal conductivity for fibers with larger M_w . Specifically, the room-temperature thermal conductivity increases from 1.2 to 4.8 W/m-K as M_w increases from 35,000 to 3,000,000. The relationship between the thermal conductivity and M_w for bulk PE was studied back in the 1960s but without much follow-up work since then. For molten PE at 140°C, it was shown that the thermal conductivity increases with M_w (roughly proportional to $\sqrt{M_w}$) and saturates as M_w approaches $\sim 140,000$.^{24,25} As Umklapp scattering becomes important at room temperature, we plot the measured thermal conductivity of the PE nanofibers at 200 K as shown in Fig. 2b, which displays a thermal conductivity escalation at a rate that is approximately proportional to $\sqrt{M_w}$. However, a notable difference is that for nanofibers, the increasing trend does not saturate until a much higher molecular weight, at $M_w > 1,000,000$ as projected from the plot. It is not surprising that the saturation regime depends on the phase of the sample (solid vs molten), as the anisotropy in the electrospun nanofiber (unlike in the stationary molten sample) allows for a greater degree of molecular orientation and thus more potential for thermal conductivity enhancement at higher

M_w . In other words, in a static molten sample, the advantages provided by high M_w are only manifested to a relatively low level due to lack of molecular orientation.

The relation between thermal conductivity and M_w for bulk isotropic polymers has been explained by a theoretical model developed by Hansen and Ho,^{24,25} and it is shown that the conductivity increase depends strongly on a parameter α , which is related to the ratio of inter-chain to intra-chain interaction strength. When this ratio goes to zero, a linear relationship between the thermal conductivity and $\sqrt{M_w}$ can be obtained. We note that Hansen and Ho indicated that, for bulk isotropic polymers, while the ratio of inter-chain to intra-chain interaction strength is quite small with $\alpha \sim 0.001$, the dependence of thermal conductivity on M_w for bulk polymers can still deviate significantly from the theoretical $\sqrt{M_w}$ dependence. For the electrospun PE nanofibers tested in this work, we applied the same theoretical model,^{24,25} and the best fit to the experimental data yielded an α value of 4×10^{-7} (Fig. 2b). This suggests that the improved chain alignment in these polymer nanofibers may enhance thermal energy transfer along the chain (relative to cross chain transfer), which leads to saturation at a higher M_w , as well as an enhanced thermal conductivity at saturation (compared to bulk amorphous PE). It is worth noting that the model was developed for bulk isotropic polymers, so the above fitting results should only be viewed as a qualitative understanding of the trend.

The temperature dependence of the thermal conductivity of electrospun PE nanofibers for different M_w also presents interesting trends. In Fig. 2a, the PE nanofibers with lower M_w (35,000 and 125,000) exhibit monotonically increasing thermal conductivity *versus* temperature, typical for amorphous materials. However, for higher M_w (420,000 and 3,000,000), a peak thermal conductivity appears as temperature increases, which is a signature of phonon Umklapp scattering occurring in crystalline solids. For fibers with a molecular weight of 420,000, the thermal

conductivity data demonstrate a $T^{-0.45}$ temperature dependence in the high temperature regime. As M_w further increases to 3,000,000, the drop rate escalates to a $T^{-0.65}$ temperature dependence, indicating increased crystallinity. Interestingly, this trend is different from what has been observed in other PE systems which have crystallized from a molten state and show decreased crystallinity at higher M_w .^{26–30}

To further understand this, we measured the crystallinity of PE nanofibers with different M_w using Raman spectroscopy.¹² Fig. 2c shows the Raman spectra of PE nanofibers with M_w of 125,000, 420,000 and 3,000,000. For low M_w PE (which is expected to contain numerous small and imperfect lamellar crystallites) the crystalline units have been shown to melt at relatively low temperature.³¹ Notably, Samuel *et al.*³² observed that small temperature increases could cause the crystalline degree of PE with $M_w = 35,000$ to drop even at temperatures slightly above room temperature. Thus, the Raman spectra of PE nanofibers with $M_w = 35,000$ are unlikely to reflect their as-fabricated crystallinity due to heating from the laser (Fig. S1); these fibers were therefore not included in this comparison. However, when the M_w is increased to 52,000, previous research indicates that PE crystallinity is insensitive to temperature until it reaches close to the melting point.³² It is well established that the Raman band at 1416 cm^{-1} is due to the orthorhombic crystalline phase of polyethylene.^{30,32–34} The CH_2 twisting vibration modes around 1300 cm^{-1} are generally used for normalization.³⁴ According to Naylor's model,³⁴ the orthorhombic crystallinity can be calculated using:

$$\% \text{ orthorhombic crystallinity} = \left(I_{1416} / I_{1300 \text{ group}} \right) \times (100 / 0.45) \times K, \quad (2)$$

where I_{1416} refers to the area of the Raman band at 1416 cm^{-1} , $I_{1300 \text{ group}}$ is the area underneath the 1300 cm^{-1} band group (internal standard), and K is a constant correction factor. As shown in Fig. 2d, the $I_{1416}/I_{1300 \text{ group}}$ ratio increases with M_w , suggesting that the electrospun PE nanofibers with

higher M_w have a larger volume fraction of orthorhombic crystalline phase, consistent with both the observed molecular weight dependence and temperature dependence of the measured thermal conductivity in Fig. 2a.

In addition to the molecular chain length, it has been predicted that the side groups in vinyl polymers may alter the vibrational properties of thermal phonons and have important effects on the thermal conductivity.^{13,35} However, to date, no systematic experimental studies have been conducted to compare the effects of side groups. As such, we also measured three other types of vinyl polymer nanofibers (PVA, PVC, and PVDF), and compared their thermal conductivities with that of PE. The four groups of vinyl polymers all have the same carbon backbone with different side groups, as described in Table 1. In considering the side group effects, we carefully select the molecular weight to ensure that the molecular chain length is similar for different vinyl nanofibers.

In a previous study, we used Raman spectroscopy to characterize the molecular chain orientation in electrospun PE nanofibers.¹² However, unlike PE, for which comprehensive Raman studies have been reported and specific parameters corresponding to different vibration modes are known and can be used to characterize the molecular chain alignment, the Raman information for the other three vinyl fibers is not as extensive. Nonetheless, we were still able to obtain some information about molecular chain alignment with polarized Raman spectroscopy on PVA, PVC, and PVDF nanofibers.

During these Raman studies, we first confirmed that laser irradiation of individual polymer nanofibers did not cause structural damage by performing the Raman spectroscopy at the same position five times in a row (Fig. S2). For PVA, PVC, and PVDF nanofibers, the intensities of the C-H stretching vibration modes at 2900 to 3000 cm^{-1} strongly depend on the angle between the incident laser polarization and the fiber axis, and the intensity reaches its maximum and minimum

at the angle of 90° and 0° , respectively. Therefore, these bands can be used to semi-quantitatively evaluate the degree of chain orientation in the nanofibers. Following the same approach as in a previous study,³⁶ we examine the parameter, $P = I_{\perp\perp} / I_{\parallel\parallel}$, as an index of the molecular orientation in the nanofibers. Here $I_{\perp\perp}$ and $I_{\parallel\parallel}$ refer to the intensities of the C-H stretching vibration modes when the polarizations of the incident and scattered laser light are perpendicular and parallel to fiber axis, respectively. As shown in Fig. 3a-c, for all PVA, PVC, and PVDF, $I_{\perp\perp}$ is stronger than $I_{\parallel\parallel}$ and the derived P values (Fig. 3d) are all around 1.5, indicating that the molecular chains are aligned along the nanofiber axis direction as a result of the strong elongational force during the electrospinning process. We note that for bulk polymers with randomly oriented molecular chains, the P value is approximately unity, as shown in Fig. S3.

The measured thermal conductivities in the temperature range of 100 K to 320 K for all four kinds of vinyl polymer nanofibers are shown in Fig. 4a. For PE, we used nanofibers with $M_w \sim 125,000$ for comparison, as this molecular weight gives a molecular chain length similar to the other three types of fibers. This way, the difference in thermal conductivity between different varieties of nanofiber is most likely due to the variation in side groups, instead of other factors. Compared to the thermal conductivities for bulk polymers (Table 1), Fig. 4a indicates that all the electrospun polymer nanofibers have enhanced thermal conductivities that are approximately 4-7 times higher than the corresponding bulk value at room temperature, again suggesting more aligned molecular chains in the electrospun nanofibers.

Fig. 4a also indicates that even though the thermal conductivity for each type of vinyl polymer fibers varies from fiber to fiber, the difference between different types of fibers is large enough to draw the conclusion that $\kappa_{PE} > \kappa_{PVA} > \kappa_{PVDF} > \kappa_{PVC}$. This represents a general trend that the thermal conductivity decreases as the side groups becomes heavier. It has been shown theoretically that

thermal phonons preferentially transport along the covalently-bonded carbon-carbon backbones in PE, and with the light hydrogen atoms as the side group, acoustic phonons in the range of 0~15 THz are the dominant heat carriers due to their high group velocities and long mean free paths.^{7,13,37} As one hydrogen atom is replaced by a heavier group (OH, Cl or F), the unit cell becomes heavier and new optical phonon mode branches with lower frequencies appear. It is generally accepted that heavier unit cells correspond to lower phonon group velocities and hence lower thermal conductivity.³⁸⁻⁴⁰ In addition, the reduced energy gap between acoustic and optical phonons may facilitate phonon Umklapp scattering to pose more resistance to thermal transport. Indeed, our experimental data are consistent with numerical modeling results showing that as the side group atomic mass increases, the acoustic phonons in the same frequency range contribute much less to thermal transport due to mismatch between the vibration modes of neighboring carbon atoms along the molecular chain.¹³ In fact, it is shown that the acoustic phonon contribution becomes very low as the side group atomic weight increases to 127 g/mol.¹³

One more observation is that, while the atomic masses of the side groups for PVDF and PVC are similar (40 g/mol *versus* 38.5 g/mol), the thermal conductivities of these two groups of nanofibers can still be quite different. In fact, the measured room-temperature thermal conductivity of PVDF nanofibers is roughly 80% higher than that of PVC nanofibers, which suggests that, in addition to the side group weight, the atomic structure or arrangement may also play a role. It is worth noting that while both α and β phases may exist in electrospun PVDF nanofibers, our Raman data indicate that the intensity of the Raman peak at 839 cm^{-1} is much stronger than that at 794 cm^{-1} (Fig. S4), suggesting that the β phase is the predominant crystal form in the fiber.⁴¹ β phase PVDF shares the same planar-zigzag carbon backbone structure as PE, PVA, and PVC, ensuring a fair comparison between these different polymer nanofibers.

When comparing the molecular structure of PVC to that of PE, one can see that, in a PVC molecule, each monomer unit has one side H atom substituted with a Cl atom. In a PVDF molecule, however, both H atoms (attached to the same C atom) are replaced by F atoms, as shown in Fig. 1a. While the details behind the reason for why the PVDF nanofibers exhibit higher thermal conductivity than the PVC nanofibers will have to be determined by future in-depth molecular modeling, we believe that the increased symmetry found in the arrangement of the F atoms in PVDF might play a role. In an earlier report, a molecular dynamics simulation on a single PE molecule indicated that the thermal conductivity drops significantly when 25% of the side H atoms are replaced by heavier F atoms (drop of 64%) or Cl atoms (drop of 66%).¹³ However, when 50% of the H atoms are replaced in a uniformly spaced arrangement, the thermal conductivity is 60% (F substitute) and 32% (Cl substitute) higher than the 25% replacement situation, respectively, indicating that symmetry plays an important role.¹³ These modeling predictions suggest that phonons travel along polymer chains more effectively when side groups are either lighter or more symmetric.

It has been shown that the Young's modulus of ultra-drawn PE fibers is much higher than bulk values, and this enhancement may correlate with significantly enhanced thermal conductivity.⁴² As such, we also examined the Young's moduli of electrospun PVA, PVC, and PVDF nanofibers and compared the results with the relative magnitude of their thermal conductivities. As we did previously for Si nanoribbons^{43,44} and polymer nanofibers,⁴⁵ the Young's modulus was characterized by performing three-point bending tests on individual suspended nanofibers using an atomic force microscope (AFM, Bruker Dimension Icon) (Fig. S5). It can be seen from Fig. 4b that different types of polymer nanofibers all demonstrate a higher Young's modulus value for smaller diameter samples, with a stronger size dependence for PVA

and PVC than that for PVDF nanofibers. In fact, similar behavior has also been observed in other polymer nanofibers,^{46–48} and the size-dependent Young's modulus could be attributed to the confinement of polymer chains near surfaces and in amorphous regions, the reduction of polymer chain entanglement, and the increase of the chain alignment for smaller sized nanofibers.^{46–49}

Moreover, as shown in Fig. 4b, the Young's moduli of the PVA nanofibers are much higher than those of the PVDF and PVC nanofibers (comparing nanofibers with similar diameters). Because the three different groups of polymer nanofibers are of the same backbone structure (planar zigzag) and similar in molecular chain length, the variations in the measured Young's modulus along the axial direction are likely due to differences in side group structure. It is known that Young's modulus is inherently related to atomic bond stiffness, and the stiffer bonds (higher modulus) observed in PVA (as compared to PVC) correlate well with the observed higher thermal conductivity. The Young's moduli of the PVDF nanofibers are, however, slightly lower than those of the PVC nanofibers, which is the opposite of the trend we observed for thermal conductivity. This is likely due to the different room temperature states for the different polymers. For semi-crystalline materials with amorphous regions, the Young's moduli will drop dramatically when the temperature increases from below to above the glass transition temperature, T_g .⁴⁶ In our experiments, the Young's moduli were all measured at room temperature, which is higher than the T_g of PVDF (-35°C)^{50,51} but lower than the T_g of PVC and PVA.^{50,52} In this case, some secondary bonds of PVDF are broken, and molecules start sliding against each other.⁵³ Thus, during the measurements, the amorphous regions in the PVDF nanofibers were in a rubbery state (whereas the PVC and PVA were in a glassy state) which is likely the reason for the relatively low Young's moduli that were measured for the PVDF nanofibers. It is worth noting that for nanofibers, T_g could be slightly different from that of the bulk; however, the shift of T_g is usually not very

significant. For example, for electrospun PVDF nanofibers with diameter from 50 nm-700 nm, T_g only increases up to -29.2°C ,⁵¹ still much lower than the room temperature at which we conducted the Young's modulus measurements.

Conclusions

In summary, we measured the thermal conductivity of individual nanofibers composed of various vinyl polymers with different molecular weights and side group atoms. Due to the fact that vibrational energy can propagate along the molecular chain more efficiently than between chains, the measured thermal conductivity increases monotonically with molecular chain length. By comparing the measured thermal conductivity of vinyl polymer nanofibers with different side groups, we found that phonons travel along polymer chains more effectively when side groups are either lighter or more symmetric. This knowledge describing the relationship between molecular structure and enhanced thermal properties in electrospun polymer nanofibers will help to better design future high-performance polymeric materials.

Acknowledgements

The authors thank the financial support from National Science Foundation (Grant# CMMI-1462866, 1462329), from NEEC (Grant# N00174-16-C-0008), and from ARO (Grant# W911NF-15-1-0441). Yin Zhang acknowledges the financial support from Natural Science Foundation of China (Grants# 51728501).

References:

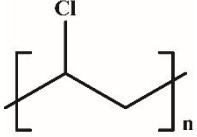
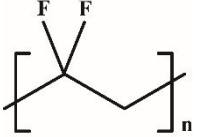
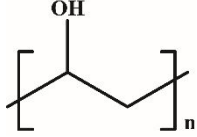
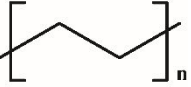
- 1 J. H. Burroughes, D. D. C. Bradley, A. R. Brown, R. N. Marks, K. Mackay, R. H. Friend, P. L. Burns and A. B. Holmes, *Nature*, 1990, **347**, 539–541.
- 2 G. Gustafsson, Y. Cao, G. M. Treacy, F. Klavetter, N. Colaneri and A. J. Heeger, *Nature*, 1992, **357**, 477–479.
- 3 M. Granström, K. Petritsch, A. C. Arias, A. Lux, M. R. Andersson and R. H. Friend, *Nature*, 1998, **395**, 257–260.
- 4 Z. He, B. Xiao, F. Liu, H. Wu, Y. Yang, S. Xiao, C. Wang, T. P. Russell and Y. Cao, *Nat. Photonics*, 2015, **9**, 174–179.
- 5 S. R. Forrest, *Nature*, 2004, **428**, 911–918.
- 6 H. Klauk, *Chem. Soc. Rev.*, 2010, **39**, 2643–2666.
- 7 A. Henry and G. Chen, *Phys. Rev. Lett.*, 2008, **101**, 235502.
- 8 S. Shen, A. Henry, J. Tong, R. Zheng and G. Chen, *Nat. Nanotechnol.*, 2010, **5**, 251–255.
- 9 V. Singh, T. L. Bougher, A. Weathers, Y. Cai, K. Bi, M. T. Pettes, S. A. McMenamin, W. Lv, D. P. Resler, T. R. Gattuso, D. H. Altman, K. H. Sandhage, L. Shi, A. Henry and B. A. Cola, *Nat Nanotechnol*, 2014, **9**, 384–390.
- 10 G.-H. Kim, D. Lee, A. Shanker, L. Shao, M. S. Kwon, D. Gidley, J. Kim and K. P. Pipe, *Nat. Mater.*, 2015, **14**, 295–300.
- 11 C. Wang, J. Guo, L. Dong, A. Aiyiti, X. Xu and B. Li, *Sci. Rep.*, 2016, **6**, 25334.
- 12 J. Ma, Q. Zhang, A. Mayo, Z. Ni, H. Yi, Y. Chen, R. Mu, L. M. Bellan and D. Li, *Nanoscale*, 2015, **7**, 16899–16908.
- 13 Q. Liao, L. Zeng, Z. Liu and W. Liu, *Sci. Rep.*, 2016, **6**, 34999.
- 14 Z. Zhong, M. C. Wingert, J. Strzalka, H.-H. Wang, T. Sun, J. Wang, R. Chen and Z. Jiang,

- Nanoscale*, 2014, **6**, 8283.
- 15 R. Shrestha, P. Li, B. Chatterjee, T. Zheng, X. Wu, Z. Liu, T. Luo, S. Choi, K. Hippalgaonkar, M. P. de Boer and S. Shen, *Nat. Commun.*, 2018, **9**, 1664.
 - 16 C. Canetta, S. Guo and A. Narayanaswamy, *Rev. Sci. Instrum.*, 2014, **85**, 104901.
 - 17 H. Ma and Z. Tian, *Appl. Phys. Lett.*, 2017, **110**, 091903.
 - 18 H. Ma, E. O'Donnell and Z. Tian, *Nanoscale*, 2018, **10**, 13924–13929.
 - 19 D. Li, Y. Wu, P. Kim, L. Shi, P. Yang and A. Majumdar, *Appl. Phys. Lett.*, 2003, **83**, 2934.
 - 20 M. C. Wingert, Z. C. Y. Chen, S. Kwon, J. Xiang and R. Chen, *Rev. Sci. Instrum.*, 2012, **83**, 024901.
 - 21 A. L. Moore and L. Shi, *Meas. Sci. Technol.*, 2010, **22**, 015103.
 - 22 Q. Zhang, Z. Cui, Z. Wei, S. Y. Chang, L. Yang, Y. Zhao, Y. Yang, Z. Guan, Y. Jiang, J. Fowlkes, J. Yang, D. Xu, Y. Chen, T. T. Xu and D. Li, *Nano Lett.*, 2017, **17**, 3550–3555.
 - 23 L. Yang, Q. Zhang, Z. Cui, M. Gerboth, Y. Zhao, T. T. Xu, D. G. Walker and D. Li, *Nano Lett.*, 2017, **17**, 7218–7225.
 - 24 D. H. and C. C. Ho, *J. Polym. Sci.*, 1965, **3**, 659–670.
 - 25 D. Hansen and B. D. Washo, *Polym. Eng. Sci.*, 1966, **6**, 260–262.
 - 26 L. J. Tung and S. Buckser, *J. Phys. Chem.*, 1958, **62**, 1530–1534.
 - 27 E. Ergoz, J. Fatou and L. Mandelkern, *Macromolecules*, 1972, **5**, 147–157.
 - 28 W. G. Perkins, N. J. Capiati and R. S. Porter, *Polym. Eng. Sci.*, 1976, **16**, 200–203.
 - 29 J. Maxfield and L. Mandelkern, *Macromolecules*, 1977, **10**, 1141–1153.
 - 30 G. R. Strobl and W. Hagedorn, *J. Polym. Sci. Polym. Phys. Ed.*, 1978, **16**, 1181–1193.
 - 31 N. S. Enikolopian, E. L. Akopian, N. M. Styrikovitch, A. S. Ketchekian and V. C. Nikolskii, *J. Polym. Sci. Part B Polym. Phys.*, 1987, **25**, 1203–1217.

- 32 A. Z. Samuel, B.-H. Lai, S.-T. Lan, M. Ando, C.-L. Wang and H. Hamaguchi, *Anal. Chem.*, 2017, **89**, 3043–3050.
- 33 C. C. Naylor, R. J. Meier, B. J. Kip, K. P. J. Williams, S. M. Mason, N. Conroy and D. L. Gerrard, *Macromolecules*, 1995, **28**, 2969–2978.
- 34 J. . Lagaron, N. . Dixon, W. Reed, J. . Pastor and B. . Kip, *Polymer*, 1999, **40**, 2569–2586.
- 35 T. Zhang, X. Wu and T. Luo, *J. Phys. Chem. C*, 2014, **118**, 21148–21159.
- 36 Z. Ma, Z. Hu, H. Zhang, M. Peng, X. He, Y. Li, Z. Yang and J. Qiu, *J. Mater. Chem. C*, 2016, **4**, 1029–1038.
- 37 J. Liu and R. Yang, *Phys. Rev. B - Condens. Matter Mater. Phys.*, 2012, **86**, 104307.
- 38 G. A. Slack, *Solid State Phys. - Adv. Res. Appl.*, 1979, **34**, 1–71.
- 39 S. Lee, K. Esfarjani, T. Luo, J. Zhou, Z. Tian and G. Chen, *Nat. Commun.*, 2014, **5**, 1–8.
- 40 W.-L. Ong, E. O'Brien, P. S. M. Dougherty, D. Paley, C. F. I. Higgs, A. J. McGaughey, H., A. J. Malen and X. Roy, *Nat. Mater.*, 2016, **16**, 83–88.
- 41 B. Mattsson, H. Ericson, L. M. Torell and F. Sundholm, *J. Polym. Sci. Part A Polym. Chem.*, 1999, **37**, 3317–3327.
- 42 P. Li, L. Hu, A. J. H. McGaughey and S. Shen, *Adv. Mater.*, 2014, **26**, 1065–1070.
- 43 L. Yang, Y. Yang, Q. Zhang, Y. Zhang, Y. Jiang, Z. Guan, M. Gerboth, J. Yang, Y. Chen, D. Greg Walker, T. T. Xu and D. Li, *Nanoscale*, 2016, **8**, 17895–17901.
- 44 Y. Calahorra, O. Shtempluck, V. Kotchetkov and Y. E. Yaish, *Nano Lett.*, 2015, **15**, 2945–2950.
- 45 L. M. Bellan, J. Kameoka and H. G. Craighead, *Nanotechnology*, 2005, **16**, 1095–1099.
- 46 A. Arinstein, M. Burman, O. Gendelman and E. Zussman, *Nat. Nanotechnol.*, 2007, **2**, 59–62.

- 47 G. Ico, A. Showalter, W. Bosze, S. C. Gott, B. S. Kim, M. P. Rao, N. V. Myung and J. Nam, *J. Mater. Chem. A*, 2016, **4**, 2293–2304.
- 48 S. Cuenot, S. Demoustier-Champagne and B. Nysten, *Elastic Modulus of Polypyrrole Nanotubes*, 2000.
- 49 M. C. Wingert, Z. Jiang, R. Chen and S. Cai, *Cit. J. Appl. Phys.*, 2017, **121**, 15103.
- 50 C. C. Ibeh, *Thermoplastic materials : properties, manufacturing methods, and applications*, CRC Press, 2011.
- 51 L. Yu and P. Cebe, *Polymer*, 2009, **50**, 2133–2141.
- 52 T. Sterzyński, J. Tomaszewska, K. Piszczek and K. Skórczewska, *Compos. Sci. Technol.*, 2010, **70**, 966–969.
- 53 C. A. Mahieux and K. L. Reifsnider, *Polymer*, 2001, **42**, 3281–3291.
- 54 J. E. Mark, *Physical Properties of Polymers Handbook*, Springer New York, New York, NY, 2007.
- 55 X. Xie, D. Li, T.-H. Tsai, J. Liu, P. V. Braun and D. G. Cahill, *Macromolecules*, 2016, **49**, 972–978.
- 56 M. Asahina and S. Enomoto, *J. Polym. Sci.*, 1962, **59**, 101–111.
- 57 K. Tashiro, *Prog. Polym. Sci.*, 1993, **18**, 377–435.
- 58 J. M. G. Cowie and I. J. McEwen, *Macromolecules*, 1977, **10**, 1124–1128.

Table 1. Properties of four vinyl polymer materials, including: formula, molecular weight (M_w), monomer weight, molecular chain length, room temperature thermal conductivity (k), calculated single chain Young's modulus ($E_{single\ chain}$), and glass transition temperature (T_g).

	PVC	PVDF	PVA	PE
Formula				
M_w	~233,000	~180,000	146,000 -186,000	~125,000
Monomer Weight	62.50	64.03	44.05	28
Chain Length	~3728	~2811	3314 - 4222	~4464
κ_{Bulk} ($W\ m^{-1}\ K^{-1}$)	0.13 ⁵⁴	0.13 ⁵⁴	0.31 ⁵⁵	0.3-0.42 ⁵⁰
κ_{Fiber} ($W\ m^{-1}\ K^{-1}$)	0.5±0.033	0.91±0.094	1.58±0.071	1.91±0.12
Density (kg/m^3)	1380	1780	1190	910-940
$E_{single\ chain}$ (GPa)	160 ⁵⁶	77(α) / 237(β) ⁵⁷	287 ⁵⁷	374 ⁴²
T_g ($^{\circ}C$)	80 ⁵²	-35 ^{50,51}	85 ⁵⁰	-78 ⁵⁸

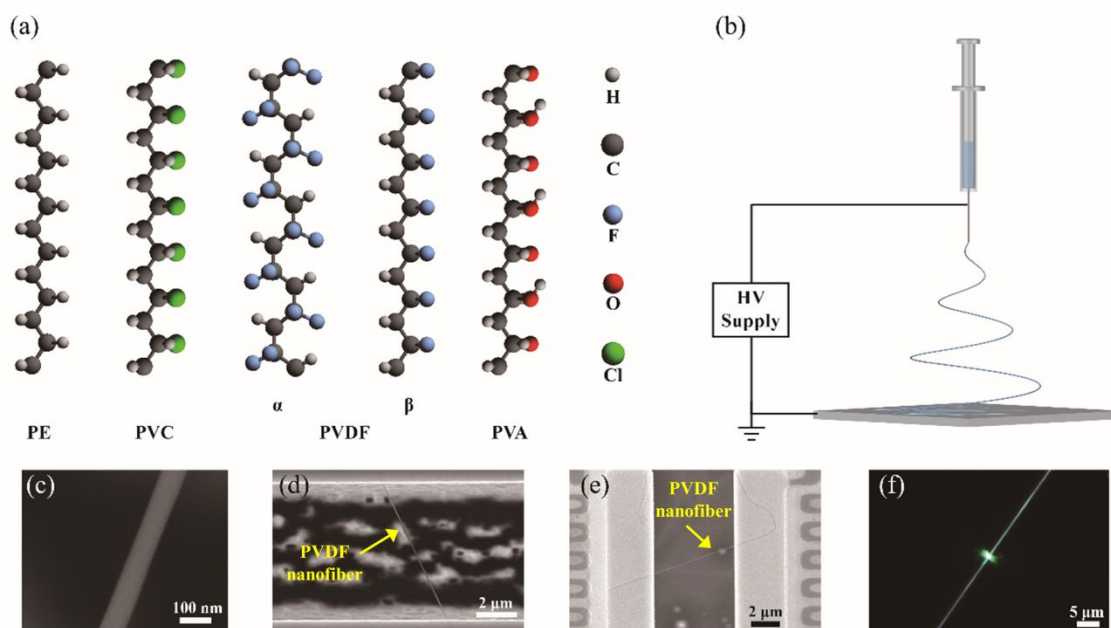


Figure 1. (a) Molecular structure of PE, PVC, PVDF (α & β phase) and PVA. (b) Schematic of electrospinning setup. (c) An SEM micrograph of a PVDF nanofiber. (d) An SEM micrograph of a PVDF nanofiber suspended over a Si trench. (e) An SEM micrograph of a PVDF nanofiber suspended on thermal measurement device. (f) Optical image showing the laser focused on individual nanofiber for Raman measurement.

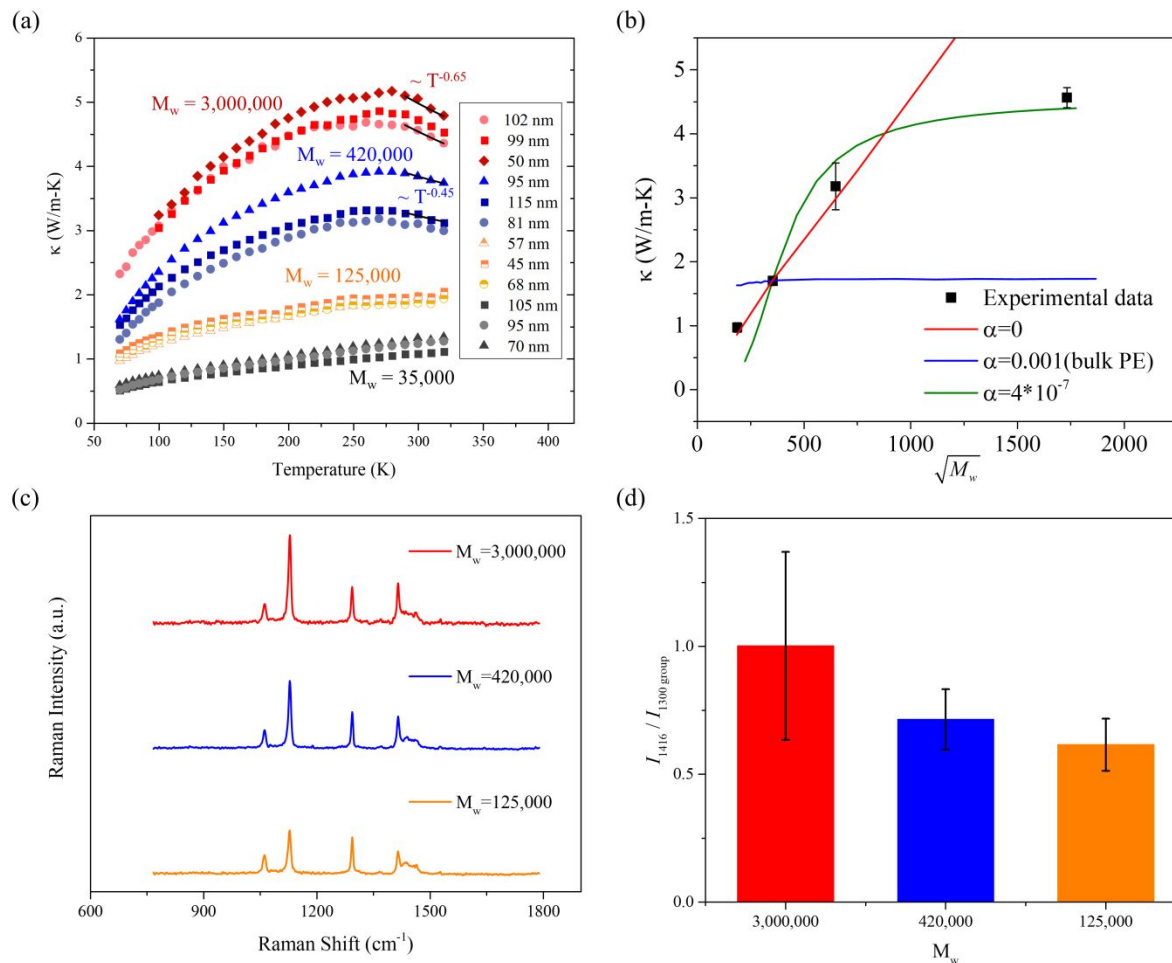


Figure 2. (a) Measured thermal conductivity of PE nanofibers with different molecular weights in the temperature range of 70–320 K. (b) Measured thermal conductivity of PE nanofibers at 200 K as a function of the square root of the molecular weight. The green curve is a fit from a model that considers the anisotropic heat flux along and across the molecular chains,^{24,25} and the red as well as blue lines are the calculated results when $\alpha = 0$ or 0.001 (bulk PE), respectively. (c) Raman spectra acquired for PE nanofibers with M_w of 3,000,000, 420,000, and 125,000, respectively. (d) The calculated intensity ratio of $I_{1416}/I_{1300 \text{ group}}$, indicating the fraction of orthorhombic crystalline phase of PE nanofibers, increases with molecular weight. The error bars indicate the standard deviation of the intensity ratio of $I_{1416}/I_{1300 \text{ group}}$ measured from several nanofibers.

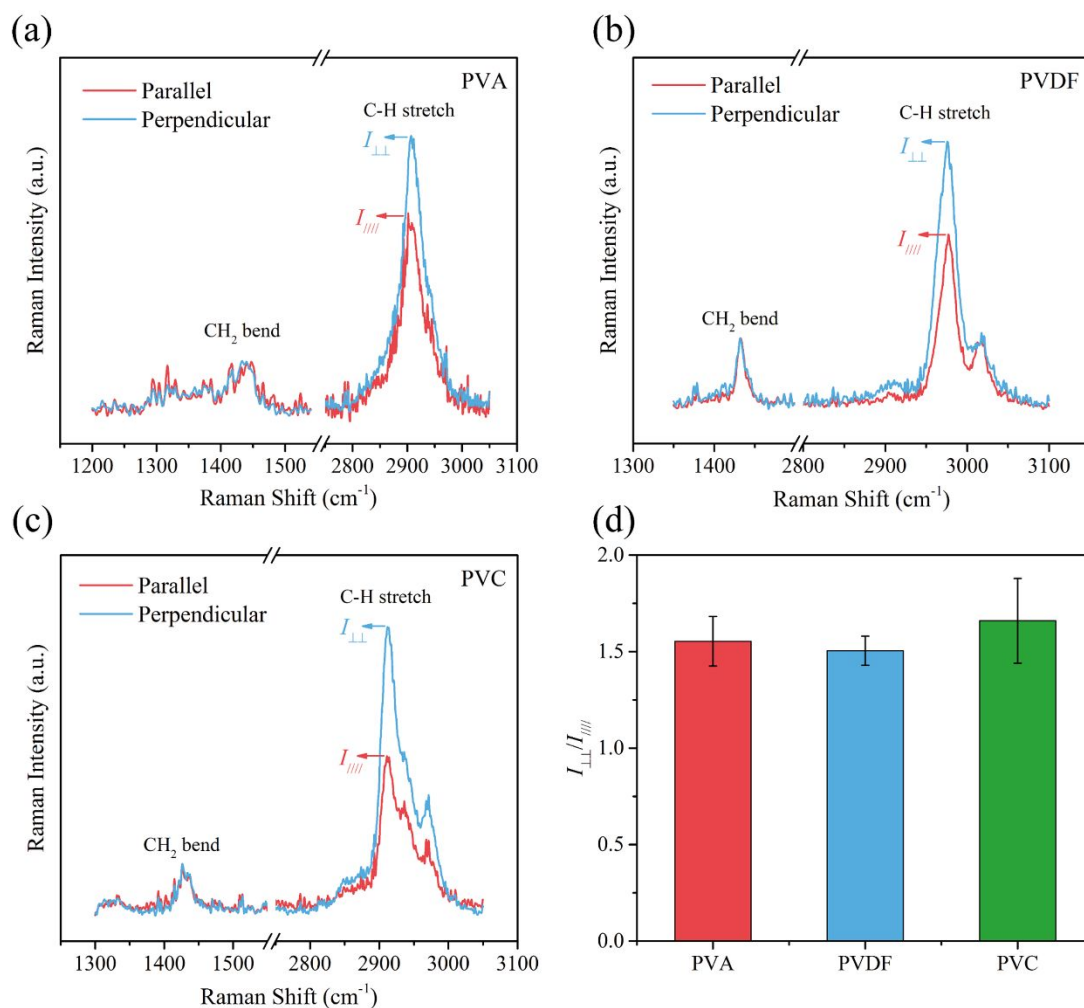


Figure 3. Polarized Raman spectra of (a) PVA, (b) PVDF, and (c) PVC nanofibers with the laser beam polarized parallel (the red curve) and perpendicular (the blue curve) to the fiber axis. (d) Values for $P = I_{\perp\perp} / I_{\parallel\parallel}$, a ratio that semi-quantitatively characterizes the molecular orientation in PVA, PVDF, and PVC nanofibers.

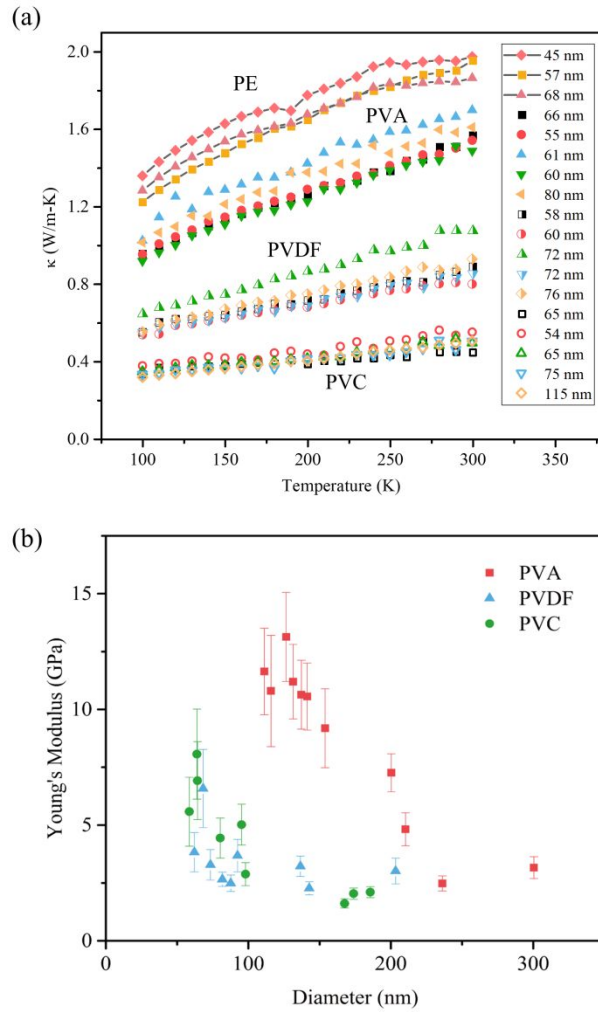
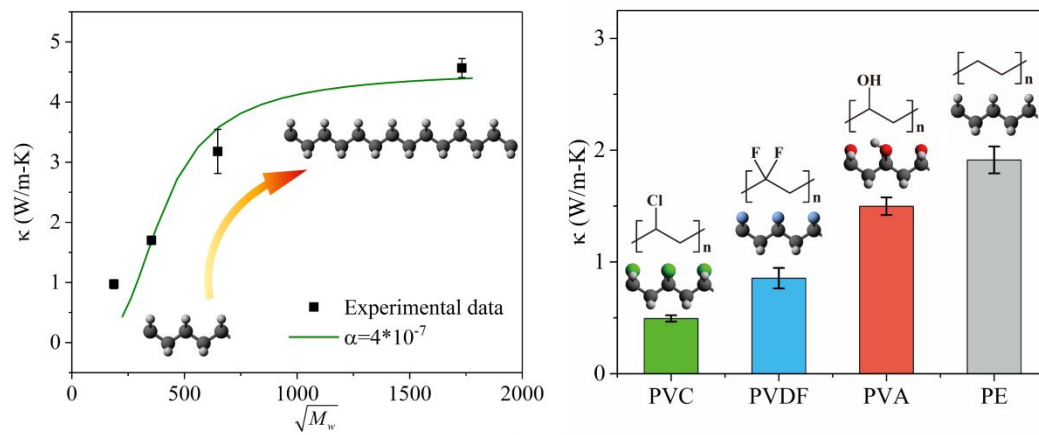


Figure 4. (a) Comparison of measured thermal conductivity of electrospun PE, PVA, PVDF, and PVC nanofibers. (b) Measured Young's moduli of PVA, PVDF and PVC nanofibers of different diameters.

TOC:



Thermal conductivity increases with molecular chain length for PE nanofibers, and is higher for vinyl polymer nanofibers with lighter and more symmetric side groups.